



## Gamma intensities for the $\beta$ -decay of $^{97}\text{Zr}$

M. Weigand<sup>a</sup>, S.F. Dellmann<sup>a</sup>, B. Brückner<sup>a</sup>, P. Erbacher<sup>a</sup>, K. Eberhardt<sup>b</sup>, C. Geppert<sup>b</sup>,  
T. Heftrich<sup>a</sup>, T. Kisselbach<sup>a</sup>, D. Kurtulgil<sup>a</sup>, M. Reich<sup>a</sup>, R. Reifarth<sup>a,c,\*</sup>, M. Volkmandt<sup>a</sup>

<sup>a</sup> Goethe University, Max-von-Laue Str. 1, Frankfurt, 60438, Germany

<sup>b</sup> Johannes Gutenberg-University, Fritz-Strassmann-Weg 2, Mainz, 55128, Germany

<sup>c</sup> University of Notre Dame, Notre Dame, IN, 46556, USA

### ARTICLE INFO

#### Keywords:

Gamma intensity

$^{97}\text{Zr}$

Beta decay

Activation

### ABSTRACT

To determine the neutron flux in activation experiments, a commonly used monitor is zirconium and in particular the stable isotopes  $^{94,96}\text{Zr}$ .  $^{96}\text{Zr}$  is very sensitive to epithermal neutrons. Despite its widespread application, most gamma intensities of the radioactive neutron capture product,  $^{97}\text{Zr}$ , yield large uncertainties. With the help of a new  $\gamma$  spectroscopy setup and GEANT simulations, we succeeded in determining a new set of  $\gamma$ -ray intensities with significantly reduced uncertainties.

### 1. Introduction

The  $\gamma$  intensities for most of the known decay  $\gamma$  radiation of  $^{97}\text{Zr}$  were re-measured in the course of a neutron activation experiment [1]. Its decay properties are relevant for neutron capture experiments at reactors and for dose estimates, since Zr is an important structure material in reactor technology.

Particularly  $^{96}\text{Zr}$  is often used as monitor isotope for neutron flux determinations because of its high sensitivity to epithermal neutrons.  $^{97}\text{Zr}$  is a short-lived isotope of zirconium, with a half-life of 16.8 h. It is produced by neutron capture on  $^{96}\text{Zr}$  and then decays completely by  $\beta^-$ -decay to  $^{97}\text{Nb}$  which is also unstable ( $t_{1/2} = 72.1$  min) and in turn decays to  $^{97}\text{Mo}$ . In the literature all known  $\gamma$  emission intensities are stated with relatively large uncertainties, with only one exception, which is the 743 keV transition. It originates from the decay of the  $^{97}\text{Nb}$  isomer which has a half-life of 53 s and decays with 100% probability via internal transition. The intensity is stated with  $(93.09 \pm 0.16)\%$  [2].

With the new  $\gamma$  spectroscopy setup [3] built up at Goethe University in Frankfurt, Germany, and by use of GEANT [4] simulations of the detector response, which will both be described in the next section, we identified discrepancies for the intensities for most other  $\gamma$ -transitions in relation to the 743 keV  $\gamma$ -ray. Thus, we can report a new improved set of  $\gamma$  intensities for the  $^{97}\text{Zr}$  decay.

### 2. Gamma spectroscopy with a head-to-head BEGe detector setup

A new detector setup for  $\gamma$  spectroscopy has been built up at Goethe University Frankfurt. It consists of two *Broad Energy Germanium* (BEGe) detectors of type BE3830 by *Mirion Technologies*, arranged in a head to head configuration as illustrated in Fig. 1. The dimensions of the

cylindrical germanium crystals are 70 mm in diameter and 30 mm in thickness. This yields a relative efficiency of about 34%. Carbon composite windows with only 0.6 mm thickness make the detectors well-suited for the use at low  $\gamma$ -ray energies. Since the detector-sample geometry has to be adjustable with respect to different sample activities and summing effects when  $\gamma$ -cascades occur, the detectors are mounted on a rail system with linear drive. This way, the distance between the sample and both detectors can be varied simultaneously in a range from about 8 mm to 130 mm. With the head to head configuration a large solid angle coverage can be achieved if a low sample activity makes it necessary. For the data acquisition NIM electronics consisting of Ortec type 672 spectroscopy amplifiers and Canberra type 8715 ADCs are used.

In order to reduce background signals from the ambient radiation field, the detector heads are enclosed in a two-component shielding. As first layer the detectors are surrounded by lead with a thickness of 100 mm. The second component inside the lead shielding is a box with 20 mm wall thickness made of copper. The copper component is important to reduce the x-ray fluorescence induced by  $\gamma$  radiation in the lead shielding. These measures result in a typical integral background count rate for the whole energy range of about 1 Hz per detector. The typical count rate spectrum of the setup is shown in Fig. 2 with the most prominent features being the 511 keV line,  $^{40}\text{K}$  and  $^{208}\text{Tl}$ . Weaker lines originate mostly from  $^{210,214}\text{Pb}$ ,  $^{214}\text{Bi}$ ,  $^{226}\text{Ra}$  and  $^{234}\text{Th}$  which are part of the Th and U decay chains. The rates of these background sources are far below the count rates of our sample and hence did not produce significant interference with the data presented in the following sections.

\* Corresponding author at: Goethe University, Max-von-Laue Str. 1, Frankfurt, 60438, Germany.

E-mail address: [reifarth@physik.uni-frankfurt.de](mailto:reifarth@physik.uni-frankfurt.de) (R. Reifarth).

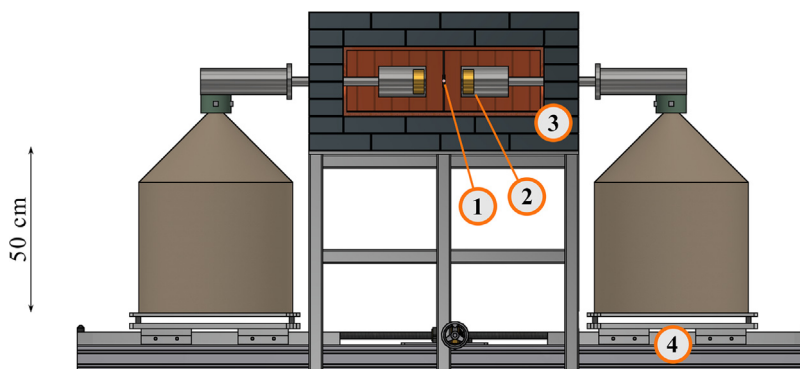


Fig. 1. Schematic view of the head-to-head detector setup with two BE3830 detectors. Labeled details: (1) Sample position, (2) Detector head with Ge crystal (yellow colour), (3) Cu/Pb shielding for the reduction of background radiation. It is drawn with an open side to give an insight. (4) Rail system with linear drive for manipulation of the sample-detector distance. The detectors are standing on adjustable base plates which allow precise alignment of the detector heads towards the sample position.

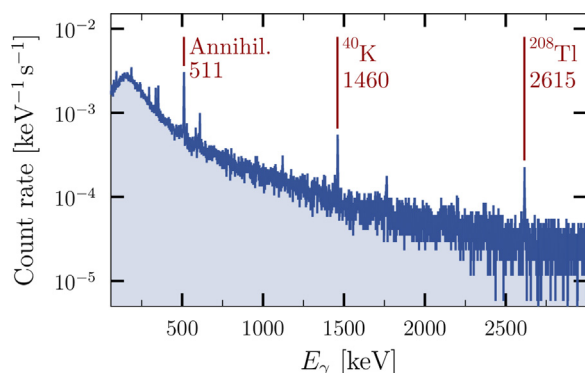


Fig. 2. Typical background rate spectrum of the BEGE  $\gamma$  spectroscopy setup with closed Pb/Cu-shielding. Some prominent  $\gamma$  lines from the remaining ambient radiation are labelled.

## 2.1. Simulation of the detector response

To understand the detector response, Monte Carlo simulations were performed with GEANT-3.21 software [4]. The following components of the setup relevant for the detection properties were considered in the simulation.

- Detection volume: Cylindrical geometry of the Ge crystals with their individual properties. Rounded edges were approximated with a chamfer. Ultra-thin dead layer were included in the simulations, which is important only at  $\gamma$ -energies below 20 keV.
- Aluminium detector housing with 1 mm thickness.
- Carbon composite window with 0.6 mm thickness.
- Sample: in case of extended samples, shape and thickness of the material were considered. Hence, absorption in the sample material is also covered by the simulation.
- Surrounding: Cu/Pb two-component shielding with their corresponding dimensions and thicknesses.
- $\gamma$ -cascades and electrons in coincidence following the  $\beta$ -decays were emitted following the actual decay schemes of the isotopes. While the  $\beta$ -spectrum followed a theoretical curve (Dirac spectrum), the  $\gamma$ -energies and intensities were based on databases (see later in text). The approach was the same as described in detail in [5].

In a first step the simulations were compared with experimental data. For this purpose, a number of calibration sources were used that cover a wide energy range and decay both under emission of single  $\gamma$ 's and via  $\gamma$ -cascades. Especially the latter case, occurring with sources like  $^{133}\text{Ba}$  where many different  $\gamma$ -rays are emitted in cascades, acts as

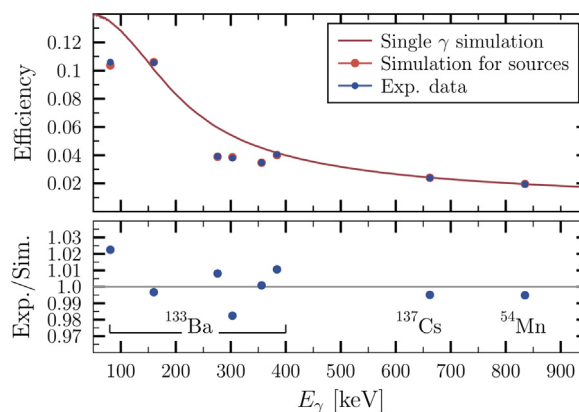


Fig. 3. Upper panel: GEANT3 simulations of the detector response for 25 mm distance between the detectors and sample position are depicted in red. The continuous line represents the efficiency for single  $\gamma$ -rays where no summing effects occur. Furthermore, the red and blue dots represent the simulated and measured efficiencies for the characteristic transitions of  $^{54}\text{Mn}$ ,  $^{137}\text{Cs}$  and  $^{133}\text{Ba}$ , respectively. Lower panel: ratio of the measured and the simulated data. The statistical uncertainties for measurement and simulation are smaller than the point size.

an important benchmark to test the reproduction of summing effects by the simulation. This is demonstrated in Fig. 3 for a distance of 25 mm between the detectors and the sample position. As the efficiency data show, summing effects of the  $^{133}\text{Ba}$  source lead to significant deviations from the single- $\gamma$  scenario, which is depicted as a continuous line. But, also visible is the good agreement between measurements and simulations with differences of 2% or less. For the later spectroscopy of  $^{97}\text{Zr}$  a larger distance of 100 mm between sample and detectors was used to further reduce summing effects to well below 1% and the accompanying uncertainties. As a follow-up test another approach was pursued to confirm the simulations over a broader energy range with a single isotope. This was also done in order to be unaffected by varying uncertainties in the activities of individual calibration sources.

## 2.2. $^{116}\text{In}$ as benchmark

Calibration sources or activated samples with many  $\gamma$ -transitions from a single isotope over a wide energy range are an ideal benchmark for the understanding of the detection efficiency and its energy dependence. For this purpose a  $^{116}\text{In}$  source ( $t_{1/2} = 54.29$  min [6]) was produced by neutron irradiation of natural indium.  $^{116}\text{In}$  offers eight  $\gamma$ -transitions from 138 keV up to 2112 keV with intensities in a useful order of magnitude and with low uncertainties. The relevant data are comprised in Table 1, along with the  $\gamma$  intensities that were observed in the GEANT simulation. These simulated intensities are the result of

**Table 1**

Energies and intensities for the relevant  $^{116}\text{In}$   $\gamma$ -transitions from literature and derived from simulated spectra (see text).

$E_\gamma$ [keV] [6]	$I_\gamma$ [%] [6]	$I_\gamma$ [%] (sim)
138.29(2)	3.70(9)	3.71
416.90(2)	27.2(4)	27.8
818.68(2)	12.13(14)	11.95
1097.28(2)	58.5(8)	58.2
1293.56(2)	84.8(12)	84.2
1507.59(2)	9.92(13)	9.99
1752.50(2)	2.36(3)	2.37
2112.29(2)	15.09(22)	15.11

starting random  $\gamma$ -cascades and electrons according to the tabulated level scheme, simulating all interactions inside the detector, counting the number of events in the peak and dividing by the nominal detection efficiency. In other words — the simulated spectra were treated like measured spectra.

For the production of the  $^{116}\text{In}$  source, protons with an energy of  $E_p = 1912$  keV impinged on a metallic Li target that was evaporated on a copper backing. This proton beam energy lies above the threshold for the  $^7\text{Li}(p,n)$  reaction leading to neutrons being emitted in a 120 degree cone behind the target [1]. A disk shaped indium sample with 20 mm in diameter and 0.2 mm thickness was placed right behind the neutron production target for about 110 min. The induced activity of  $^{116}\text{In}$  was then measured at the BEGe detector setup with the distance between detectors and sample set to 100 mm. This is far enough to ensure a low probability for summing effects. The remaining influence of coincident signals from  $\gamma$ -cascades is considered within the framework of the GEANT simulations.

On one hand, the spectroscopy of  $^{116}\text{In}$  allows the detector response of both detectors to be compared. The data show good agreement between the two detectors within the given statistical uncertainties. The result of the analysis is depicted in Fig. 4 (b). The 1752 keV transition stands out with comparably large uncertainties due to its low intensity which results in lower statistics.

On the other hand, the quality of the GEANT3 simulation of the detector setup could be tested over a broad energy range. This was done by calculating the ratio of the measured count numbers to the simulated count numbers. For the resulting distribution shown in Fig. 4 (c) the weighted average of the ratios of all lines was calculated and used for normalization. If the simulation would wrongly represent the detector response to the  $^{116}\text{In}$  decay, significant deviations would become visible here. The depicted uncertainties consider the statistical uncertainties of the measurement and simulations, as well as the uncertainties of the  $\gamma$  intensities. The fluctuations around the weighted average delivers an uncertainty for the GEANT3 simulation of 0.4%.

### 3. Determination of the $^{97}\text{Zr}$ gamma intensities

The determination of the  $\gamma$  intensities for the  $^{97}\text{Zr}$  decay followed essentially the same procedure as for the  $^{116}\text{In}$ . Zr sample material with sufficiently high activity had to be produced, followed by  $\gamma$  spectroscopy and GEANT3 simulations. Those steps are described in the following sections.

#### 3.1. Zr activation at TRIGA Mainz

Neutron activation of  $^{96}\text{Zr}$  was performed in the research reactor TRIGA in Mainz [7]. The samples were placed in the rotary specimen rack surrounding the reactor core. The continuous movement around the reactor core delivers a uniform irradiation of the sample. The typical neutron flux at this position is  $0.7 \cdot 10^{12}$  n cm $^{-2}$  s $^{-1}$  for thermal neutron flux and  $4 \cdot 10^{10}$  n cm $^{-2}$  s $^{-1}$  for epithermal flux. The samples were irradiated for 3 h.

The originally intended use of the Zr samples was as flux monitors. Flux monitors are samples whose effective cross sections are well

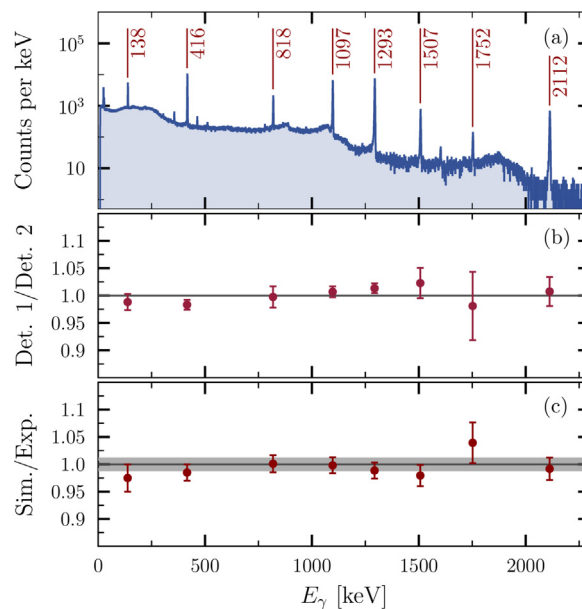


Fig. 4. (a)  $^{116}\text{In}$  data measured with one of the detectors.  $\gamma$ -transitions used in the analysis are labelled with their energies in keV. (b) Comparison of the measured detector response of both detectors based on the  $^{116}\text{In}$  data for each line with statistical uncertainties. (c) The normalized ratio of the measured and the simulated counts for each  $^{116}\text{In}$  line. The data are normalized to the weighted average of all ratios with its uncertainty shown as grey area.

known, hence allowing the determination of the neutron fluence. To determine both the thermal cross section and the resonance integral of the investigated sample, the cadmium difference method was used. In this method, the sample is irradiated a second time, shielded with a cadmium layer. This layer leads to a strong absorption of thermal neutrons, since the isotope  $^{113}\text{Cd}$  has a large neutron capture cross section in this energy range. As a result, almost all epithermal neutrons can penetrate the cadmium, and below an energy threshold of about 0.5 eV, thermal neutrons are strongly absorbed. Since  $^{96}\text{Zr}$  has a relatively large resonance integral, it was still possible to obtain good statistics for  $\gamma$ -ray spectroscopy of  $^{97}\text{Zr}$  despite the shielding. In this experiment, zirconium was activated with weights of about 0.02 g for the first activation and with weights of about 0.008 g for the second activation with cadmium shielding, each with a thickness of 0.1 cm.

#### 3.2. Gamma spectroscopy of $^{97}\text{Zr}$

The spectroscopy of  $^{97}\text{Zr}$  was performed at the BEGe setup introduced before. The analysis is hampered by different factors. Firstly, there is a huge difference in terms of  $\gamma$  intensities between the dominating 743 keV transition, producing a strong Compton background for lines at lower energies. Secondly, the  $^{97}\text{Zr}$  decay also introduces a broad background component due to the  $\beta^-$  radiation with an endpoint energy of 1.9 MeV. This affects the analysis of almost all the observed  $\gamma$  lines of  $^{97}\text{Zr}$ . Another important component are the spectral features of  $^{97}\text{Nb}$  — including another  $\beta^-$  radiation component with an endpoint energy of 1.3 MeV — which inevitably accompany those of  $^{97}\text{Zr}$ . Since  $^{97}\text{Nb}$  has a shorter half-life of only 72.1 min, equilibrium was quickly reached before the measurements [2]. Hence, during the measurements, its  $\gamma$  rates were determined by the  $^{97}\text{Zr}$  decay rate with the 657.94 keV line being the dominating feature. This line also introduces a significant Compton background for the  $^{97}\text{Zr}$  lines at lower energies.

These strong background components together hamper the analysis of weak  $\gamma$  lines. This is demonstrated for one data set in Fig. 5 (c) for the 202.5 keV line ( $I_\gamma = 0.029(8)\%$  according to [2]), where the

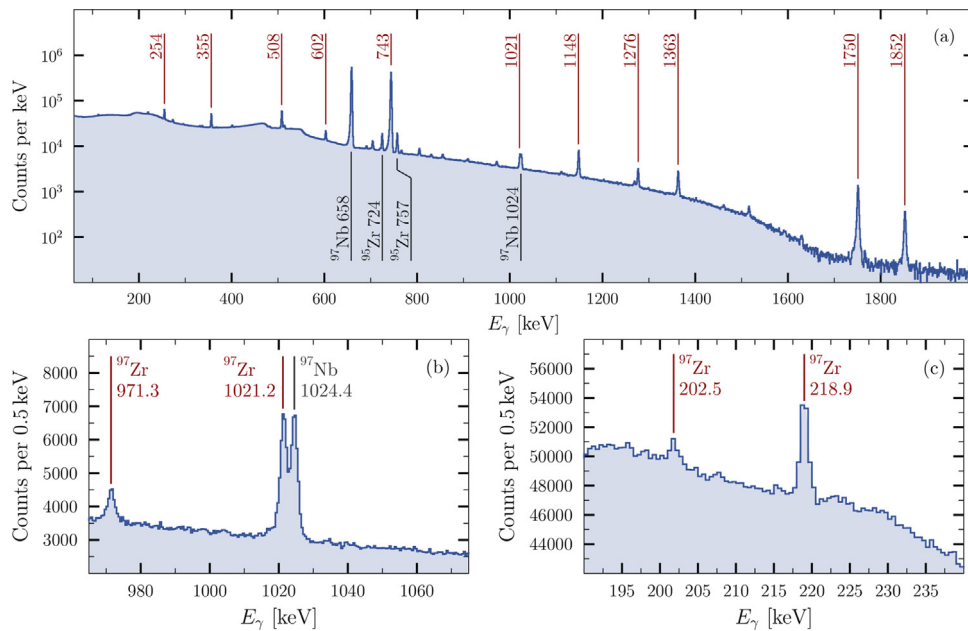


**Fig. 5.** These spectra show the sum over all data collected with both detectors and two samples from one activation campaign. Relevant lines are labelled with their energies in keV. (a) Overview spectrum for the  $^{97}\text{Zr}$  measurement. The most prominent features of  $^{97}\text{Zr}$  are labelled in red. Sample induced background features are labelled in black. (b) Detail view of the 1021.2 keV line from  $^{97}\text{Zr}$  from one of the two acquired data sets. It partially overlaps with the 1024.4 keV line from  $^{97}\text{Nb}$ . (c) One of the weakest transitions of  $^{97}\text{Zr}$  at 202.5 keV ( $I_\gamma = 0.029(8)\%$ ) that could be analysed. Despite having a reasonable number of counts in the peak, the strong background causes large uncertainties.

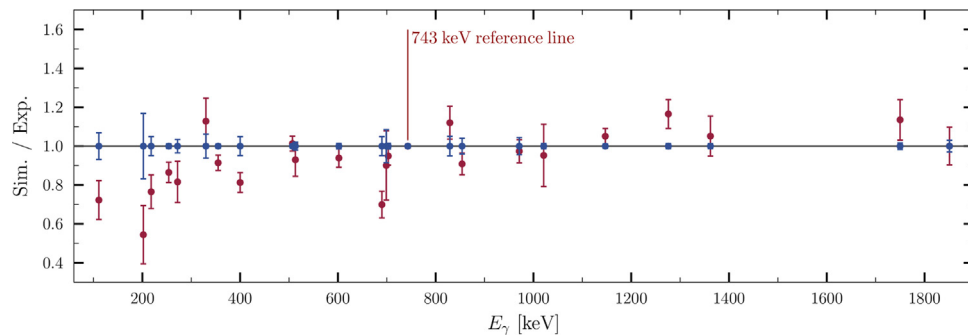


**Fig. 6.** Comparison of the simulated detector response to the  $^{97}\text{Zr}$  decay with the measured data (red). The distribution was normalized to one for the 743 keV transition which acts as reference because of its low uncertainty. The uncertainties originate from the  $\gamma$  intensities stated in the NNDC database. The blue data point depicts the resulting uncertainties for the corrected  $\gamma$  intensities.

peak contains several thousand counts, but the high background level still leads to an uncertainty of 16.8% for the new  $\gamma$  intensity. For each line the background is described by a linear model based on the data adjacent left and right to the corresponding peak. The peak contents were determined by integration and subtraction of the background contribution. Although it is in principle possible to reduce the number of decay-electrons reaching the detector using low-Z absorbers, we decided against it, since it also affects the low-energy  $\gamma$ -rays and introduced secondary background from high-energy  $\gamma$ -rays interacting in the absorber.

Only in the case of double peak structures like the  $^{97}\text{Zr}$  1021.2 keV line Gaussian profiles had to be fitted in order to obtain count numbers from the peak of interest. This example is depicted in Fig. 5 (b). The double peak nature is caused by the 1024.4 keV line from  $^{97}\text{Nb}$  which is always present in  $^{97}\text{Zr}$  spectra as described before.

Data sets from two different reactor activations were obtained, one time with and the other time without cadmium shielding. For the spectroscopy of all samples the sample-detector distance was set to 100 mm as for the  $^{116}\text{In}$  measurements. The data were measured with different gain settings. Higher gain settings were used to achieve a good resolution in the lower energy regime. For the second data set a lower

gain setting was used to also cover the two  $^{97}\text{Zr}$  lines at 1750.24 keV and 1851.61 keV.

### 3.3. New gamma intensities

For the determination of the new  $\gamma$  intensities the  $^{97}\text{Zr}$  decay was also simulated in GEANT3 and compared with the spectroscopic data. For all the observed lines the ratios of measured counts versus simulated counts were determined and then normalized such that the ratio for the 743 keV line equals 1 (see Fig. 6). Hence the new values are determined relative to the intensity of this transition, see Table 2. This way new intensities for 23  $\gamma$ -transitions could be determined with lower uncertainties than stated in the literature. Only some of the weakest transitions of  $^{97}\text{Zr}$  recorded in the NNDC database could not be observed. This might be due to the strong background components or background in previous measurements.

## 4. Summary

A re-measurement of the  $\gamma$  intensities of the isotope  $^{97}\text{Zr}$  has been successfully performed within an activation experiment at the TRIGA

**Table 2**

Literature and newly measured  $\gamma$  intensities. All intensities are per decay. The transition with 743.36 keV was used as a reference (see text).

$E_\gamma$ [keV] NNDC [2]	$I_\gamma$ [%] NNDC [2]	$I_\gamma$ [%] This work
111.6	0.065(9)	0.090(6)
182.9	0.032(7)	Not observed
202.5	0.029(8)	0.053(9)
218.9	0.168(19)	0.218(11)
254.17	1.15(7)	1.330(16)
272.4	0.23(3)	0.283(10)
297.2	0.066(11)	Not observed
305.1	0.028(19)	Not observed
330.43	0.143(15)	0.126(8)
355.4	2.09(9)	2.285(24)
400.42	0.245(16)	0.299(15)
473.5	0.07(4)	Not observed
507.64	5.03(19)	5.033(47)
513.41	0.55(5)	0.588(12)
558	0.028(19)	Not observed
600.6	0.09(9)	Not observed
602.37	1.38(7)	1.468(21)
690.52	0.183(18)	0.262(13)
699.2	0.101(20)	0.112(10)
703.76	1.01(5)	1.013(15)
707.4	0.032(17)	Not observed
<b>743.36</b>	<b>93.09(16)</b>	<b>93.09(16)</b>
829.79	0.239(18)	0.213(11)
854.89	0.357(22)	0.392(16)
971.34	0.278(17)	0.287(13)
1021.2	1.01(17)	1.062(15)
1147.97	2.62(10)	2.462(27)
1276.07	0.94(6)	0.812(11)
1362.68	1.02(10)	0.975(13)
1750.24	1.09(10)	0.959(16)
1851.61	0.31(3)	0.289(9)

reactor in Mainz, Germany. The  $\gamma$  spectroscopy was performed at a new detector setup at the Goethe University Frankfurt. The setup consists of two BEGe detectors, which are arranged in a head to head configuration. In combination with thoroughly tested GEANT simulations the new  $\gamma$  intensities could be determined. Overall, a newly measured set of intensities of 23  $\gamma$ -transitions was established. Previously, these values were dominated by large uncertainties, which could be reduced significantly.

## Declaration of competing interest

The authors declare that they have no known competing financial interests or personal relationships that could have appeared to influence the work reported in this paper.

## Data availability

No data was used for the research described in the article.

## Acknowledgements

This project was supported by GIF grant I-1500-303.7/2019, HGS-HIRE, HFHF. RR acknowledges support by the Glynn family. We thank the operators at the TRIGA reactor Mainz for their excellent support. We also thank the operators of the van de Graaff accelerator at the IKF at Goethe University Frankfurt, M. Dworak and P. Ziel.

## References

- [1] R. Reifarh, P. Erbacher, S. Fiebiger, K. Göbel, T. Heftrich, M. Heil, F. Käppeler, N. Klapper, D. Kurtulgil, C. Langer, C. Lederer-Woods, A. Mengoni, B. Thomas, S. Schmidt, M. Weigand, M. Wiescher, Neutron-induced cross sections - from raw data to astrophysical rates, *Eur. Phys. J. Plus* 133 (2018) 424.
- [2] N. Nica, Nuclear data sheets for a=97, *Nucl. Data Sheets* 111 (3) (2010) 525–716.
- [3] R. Reifarh, L. Bott, B. Brückner, O. Dogan, M. Dworak, A. Endres, P. Erbacher, S. Fiebiger, R. Gernhäuser, K. Göbel, F. Hebermehl, T. Heftrich, C. Langer, T. Kausch, N. Klapper, K. Khasawneh, C. Köppchen, S. Krasilovskaja, D. Kurtulgil, M. Reich, M.S. Schöffler, L.P.H. Schmidt, C. Schwarz, Z. Slavkovská, K.E. Stiebing, B. Thomas, M. Volkandt, M. Weigand, M. Wiescher, P. Ziel, Investigation of neutron-induced reaction at the goethe university frankfurt, in: *Nuclei in the Cosmos XV*, Vol. 219, 2019, pp. 253–257, [http://dx.doi.org/10.1007/978-3-030-13876-9\\_42](http://dx.doi.org/10.1007/978-3-030-13876-9_42), arXiv:1905.05584.
- [4] J. Apostolakis, Cern Program Library Long Writeup, W5013, Tech. Rep., CERN, GEANT library, 1993, <http://wwwinfo.cern.ch/asd/geant/>.
- [5] A. Couture, R. Reifarh, Direct measurements of neutron capture on radioactive isotopes, *At. Data Nucl. Data Tables* 93 (2007) 807.
- [6] J. Blachot, Nuclear data sheets for a=116, *Nucl. Data Sheets* 111 (3) (2010) 717–895.
- [7] K. Eberhardt, C. Geppert, The research reactor triga mainz – a strong and versatile neutron source for science and education, *Radiochim. Acta* 107 (7) (2019) 535–546, <http://dx.doi.org/10.1515/ract-2019-3127>, [cited 2022-08-17].